

## Particle Distribution Analysis on Stainless steel - Aluminum Dispersion Plate

Hyeong-Jin Kim, Ho Jin Ryu\*,

Department of Nuclear and Quantum Engineering, KAIST, Daehak-ro 291, Yuseong-gu, Daejeon, 34141, Korea

\*Corresponding author: hojinryu@kaist.ac.kr

### 1. Introduction

Tc-99m is the most commonly used radioisotope for millions of medical diagnoses. The main source of Tc-99m is Mo-99, extracted from fission products of the research reactors [1]. After non-proliferation policy claims to minimize the use of highly enriched uranium (HEU) in medical radioisotope production, researchers have dedicated to developing low enriched uranium (LEU) targets to replace the conventional HEU targets. However, due to the low fissile element content, LEU target has lower Mo-99 production efficiency. In order to improve the productivity of radioisotope, it is necessary to develop LEU targets with high-uranium-density [2].

Centrifugal atomization technique is one of the innovative approaches to developing high-uranium density LEU targets, which is effective for the production of uranium alloy powders. U-Al dispersion plates up to  $9.0 \text{ gU/cm}^3$  density were fabricated based on centrifugal atomization [3], and the metallurgical reaction between U-Al during fabrication process was investigated [4].

The interaction layer (IL) consists of intermetallic compound  $\text{UAl}_x$ , is formed during the fabrication process. Since IL has a low density which leads to a volumetric increase, degradation of thermal properties can occur. Larger fuel sizes lower the volume fraction of IL, but for larger particle sizes, fuel particle clustering can occur during the fabrication process. In order to obtain the desirable particle distribution, optimized fabrication conditions should be set by analyzing the 3D microstructure of the dispersion target.

In this study, methodology to figure out the fuel particle homogeneity with application of x-ray based computer-aided tomographic process was established.

### 2. Methodology

Stainless steel-aluminum dispersion plate was fabricated using atomized stainless steel powder, and the internal information was obtained by computed tomography (CT).

#### 2.1. Fabrication of stainless steel-aluminum dispersion plate

Uranium fuel element was replaced by stainless steel with a density of  $8.03 \text{ g/cm}^3$ . Stainless steel powder was prepared by centrifugal atomization and sieved to 50-150  $\mu\text{m}$  grade. The sieved powder then mixed with aluminum powder, and compacted using the bi-axial press.

#### 2.2. Data acquisition by micro-CT imaging

Table I: Specification of CT used for data acquisition

Max power	Energy range	Normal resolution
10 W	40~100 kV	0.45 $\mu\text{m}$

The fabricated sample was then observed by micro-CT. CT has two main advantages: first, SEM shows only a cross-sectional image of the partial internal structure, while CT can describe the entire internal structure. Second, the CT imaging process is a non-destructive test, which does not damage the test specimen. Table I shows the specification of CT used for data acquisition. The resolution is appropriate for observing particle sizes of about 100  $\mu\text{m}$ .

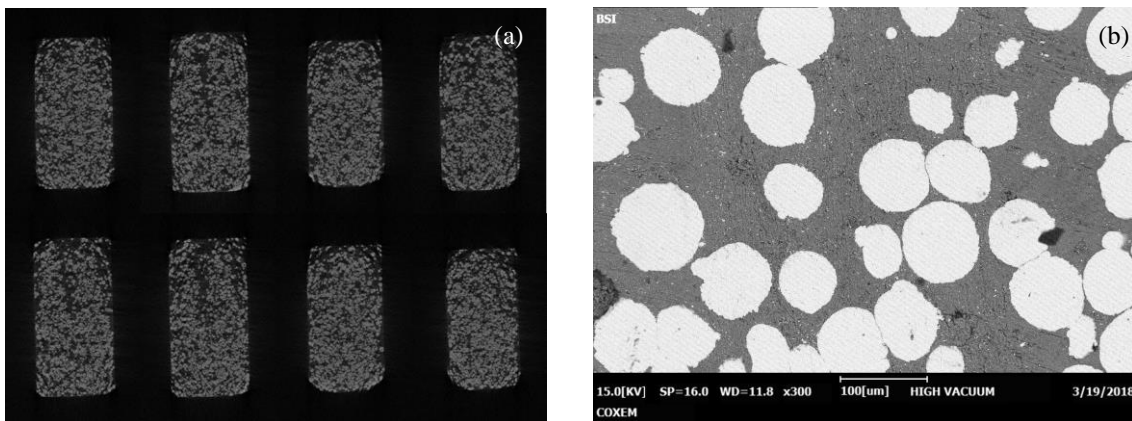


Fig. 1. Cross-sectional image of SS-Al dispersion plate, observed by (a) micro-CT and (b) SEM

### 3. Results

#### 3.1. CT cross-sectional image

Cross-sectional image of fabricated samples was obtained by micro-CT as shown in Fig. 1. (a). We found that x-ray energy was suitable to penetrate the sample, and the density difference between stainless steel and aluminum was sufficient to distinguish on the image. Referring to the cross-sectional image obtained by SEM (Fig. 1. (b)), the CT image has fully implemented the microstructure of the target.

#### 3.2. Processed image

Two steps of image processing for data manipulation were executed using the MATLAB platform. First, we used Gaussian blur to remove noise from the image. The standard deviation value was chosen as 3 pixels. Then, a threshold value was set so that stainless steel and aluminum would be separated into black and white images. Whole image processing procedure is demonstrated in Fig. 2.

#### 4.3. Particle homogeneity calculation

Data manipulation was also performed using MATLAB platform. In order to analyze the two-phase heterogeneous system, the following method was used. First, in the 3D stacked image, “cell” which is a cube-shaped region to be calculated, defined by the number of pixels on one side, was set. Then the volume fraction of stainless steel inside the cell was calculated while cell position was randomly changed inside the stacked image. The calculated volume fraction was then plotted against cell size.

The fast convergence denotes the uniform particle distribution, while the slower convergence implies the presence of clusters of particles. Fig. 3 shows a convergence graph calculated from the processed data of the fabricated sample. This graph shows convergence pattern as expected, and we concluded that the methodology for particle distribution analysis is valid.

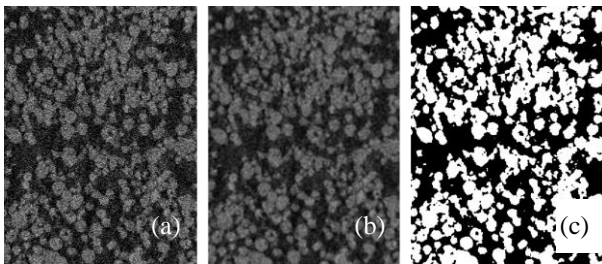


Fig. 2. (a) Raw image (b) Gaussian blurred image (c) B/W image with threshold value.

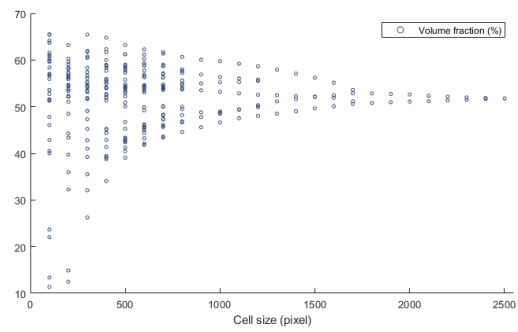


Fig. 3. The volume fraction of stainless steel plotted according to an increase in cell size

### 4. Conclusions

It was confirmed that the CT technique is suitable for observing the fabricated stainless steel – aluminum dispersion sample.

Image processing was performed on the obtained CT image, and data processing was performed to calculate the volume fraction of stainless steel particles. The resulting graph shows that the volume fraction converges according to the cell size, and the degree of convergence represents the homogeneity of internal particles.

### Acknowledgment

This work was supported by the National Research Foundation of Korea (NRF, No. 2018M2A8A1023313) funded by the Ministry of Science, ICT and Future Planning.

### REFERENCES

- [1] van der Marck SC, Koning AJ, and Charlton KE, The options for the future production of the medical isotope  $^{99}\text{Mo}$ , *Eur J Nucl Med Mol Imaging*, Vol. 37, pp. 1817-1820, 2010.
- [2] Pillai MRA, Dash A, and Knapp FR, Sustained availability of  $^{99m}\text{Tc}$ : possible paths forward, *J Nucl Med*, Vol. 54, pp. 313-323, 2013. pp. 612-613, 1999.
- [3] Ryu, H. J., Kim, C. K., Sim, M., Park, J. M., and Lee, J. H., Development of high-density U/Al dispersion plates for Mo-99 production using atomized uranium powder. *Nucl. Eng. Technol.* Vol. 45, pp. 979–986, 2013.
- [4] Ryu, H. J., Jeong, Y. J., Nam, J. M. and Park, J. M., Metallurgical considerations for the fabrication of low-enriched uranium dispersion targets with a high density for  $^{99}\text{Mo}$  production, *J. Radioanal. Nucl. Chem*, Vol. 305, pp. 31-39, 2015.